Controlling Nanoantenna Polarizability through Backaction via a Single Cavity Mode

Freek Ruesink,[1] Hugo M. Doeleman,[2,1] Ewold Verhagen,[1] and A. Femius Koenderink[1,2,*]
[1]*Center for Nanophotonics, AMOLF, Science Park 104, 1098 XG Amsterdam, The Netherlands*
[2]*Van der Waals-Zeeman Institute, University of Amsterdam, Science Park 904, PO Box 94485, 1090 GL Amsterdam, The Netherlands*

(Received 18 December 2017; published 17 May 2018)

The polarizability α determines the absorption, extinction, and scattering by small particles. Beyond being purely set by scatterer size and material, in fact polarizability can be affected by backaction: the influence of the photonic environment on the scatterer. As such, controlling the strength of backaction provides a tool to tailor the (radiative) properties of nanoparticles. Here, we control the backaction between broadband scatterers and a single mode of a high-quality cavity. We demonstrate that backaction from a microtoroid ring resonator significantly alters the polarizability of an array of nanorods: the polarizability is renormalized as fields scattered from—and returning to—the nanorods via the ring resonator depolarize the rods. Moreover, we show that it is possible to control the strength of the backaction by exploiting the diffractive properties of the array. This perturbation of a strong scatterer by a nearby cavity has important implications for hybrid plasmonic-photonic resonators and the understanding of coupled optical resonators in general.

DOI: 10.1103/PhysRevLett.120.206101

The scattering, absorption, and extinction cross section of small scatterers is often attributed to the dielectric properties of the particle, i.e., the scatterer's volume, shape, and its refractive index with respect to the host medium [1]. Central to this argument, for scatterers with a physical size much smaller than the wavelength, is the so-called *polarizability*, which contains the frequency-dependent susceptibility that quantifies the strength of the dipole moment induced in the scatterer by an incident field. A rather subtle notion is that the polarizability also depends on the mode structure offered by the photonic environment (Fig. 1). To illustrate this, consider that extinction, i.e., the total power that a scatterer extracts from an incident beam [1] is directly proportional to the imaginary part of polarizability. According to the optical theorem [2], this power is distributed over Ohmic heating and scattering, with the contribution of scattering being proportional to the squared magnitude of polarizability and the local density of states (LDOS) [3]. The fact that LDOS, i.e., the number of available photonic modes for the scatterer to radiate into, enters the polarizability is known as backaction: a correction on the total field that drives a polarizable scatterer. This correction is neglected in standard (Rayleigh) scattering theory [1]. However, even for a single scatterer placed in free space, backaction leads to additional damping (depolarization) and thus needs to be integrated in a self-consistent description of any system [2,4]. Although backaction effects on quantum emitters [5] have been routinely studied, very few studies exist that probe backaction on plasmonic scatterers. First, Buchler *et al.* [6] revealed that the spectral width of a nanoantenna's plasmon resonance can be modulated when the antenna approaches a reflector, whereas more recently Heylman *et al.* [7] demonstrated that the absorption cross section of a single nanoantenna can be modified via coupling to a microtoroid cavity. While backaction on a single antenna is perhaps the most intuitive example to study, one is not limited to a *single* antenna or resonator to observe backaction. For any resonating system that is coupled to a bath of modes, the properties of this bath will influence the susceptibility (polarizability) of the resonating system. Crucially, this change in susceptibility caries information on the properties of the bath, and a measurement of the modified susceptibility thus provides a noninvasive method to obtain information on the bath. It has been proposed [8] that if the bath is represented by the single mode of a cavity, the modified susceptibility would, in principle, allow access to the Purcell factor [9] of the cavity mode.

Here we experimentally investigate backaction on polarizability in a hybrid cavity-antenna system [Fig. 2(a)],

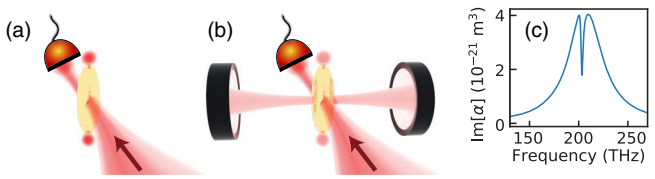

FIG. 1. (a) Single polarizable scatterer. (b) A simple Fabry-Pérot cavity modifies the local density of states and alters the scattering properties of a plasmonic scatterer. (c) A spectrally narrow cavity mode can suppress the imaginary part of the polarizability of a plasmonic scatterer.

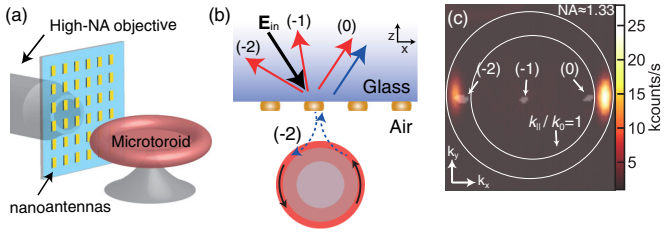

FIG. 2. (a) Cartoon of the hybrid cavity-antenna system. (b) For some incoming field $\mathbf{E}_{in}$, the (-2) diffraction order associated with the array evanescently couples to the toroid. Backaction from the cavity on the array is measured in the specular reflection signal. We block the (-2) and (-1) diffraction orders back into the glass, as well as direct radiation of the cavity into the glass substrate. (c) An overlay of Fourier images obtained via back focal plane imaging. The transparent white blobs indicated by arrows are diffraction orders. The (-2) order overlaps with one of the cavity modes (indicated with the color scale), exciting the cavity mode via the antenna array.

demonstrating a strongly modified extinction response of an array of gold nanorods due to backaction imparted by a single whispering-gallery mode (WGM) of a microtoroid ring resonator. At conditions where the cavity offers a high mode density for the scatterers to radiate into, the nanorods' susceptibility to an incoming field is suppressed: the cavity mode density thus effectively depolarizes the nanorods [Fig. 1(c)], yielding an experimental signature that relates to electromagnetically induced transparency [10]. A unique feature of the array, as our experiments reveal, is that it is possible to control the strength of the measured backaction by careful tuning of a diffraction order of the array, phase matching its wave vector with the WGM of the cavity. Using a coupled-oscillator model we retrieve an antenna-cavity cooperativity and provide a lower bound on the cavity Purcell factor [9] at the lattice origin. Our results have large relevance in the context of recent proposals on hybrid plasmonic-photonic resonators [8,11–19] as a unique venue for huge Purcell factors [9] and quantum strong coupling with single emitters. While the most intuitive consideration for such a proposal is to assess how scatterers perturb cavity resonances [20], in fact, this work shows that one rather has to ask what opportunities the cavity offers to control antenna polarizability.

An ideal experiment to probe cavity-induced backaction would directly measure the complex-valued polarizability α in presence and absence of the microtoroid. This is not a trivial task: polarizability is not a directly measurable quantity in optics. Instead one has to rely on far-field measurements of extinction and scattering cross sections to deduce $\mathrm{Im}[\alpha]$ and $|\alpha|^2$ respectively. Such quantitative polarizability measurements are challenging even for scatterers in a uniform environment [21,22]. The proximity of the cavity further complicates the task of strictly probing the scatterers only. Practically, this means that direct excitation of the cavity mode by the incident beam, as well as radiation from the cavity directly into the detection channel, should be prevented, as both would contaminate the interrogation of the scatterer's response. We approach these constraints by a combination of experimental techniques. First, we use a WGM resonator that only allows in- and outcoupling of light under select wave vector matching conditions. Second, we use an array of antennas, as opposed to a single antenna, to obtain a strong extinctionlike signal that can be probed in specular reflection with a nearly collimated plane wave, again using wave vector conservation to separate the extinction channel from all other scattering channels. Crucially, the use of an array allows tailoring of the coupling strength between cavity and array via wave vector matching, controlled by the angle of incidence. Note that our choice for an array results in a measurement probing backaction on the *lattice* polarizability [23].

We use gold nanorods with length (width) of 400 nm (120 nm) and thickness of 40 nm placed on a glass substrate in an array with 800 (1500) nm pitch along the long (short) axis of the rods. In absence of the cavity, the array exhibits a broadband resonant response centered at $\omega_a/2\pi \approx 208$ THz [20,24] (linewidth $\gamma \approx 55$ THz), while the microtoroid [31] (linewidth $\kappa \approx 30$ MHz) is resonant at slightly red-detuned frequency $\omega_c/2\pi \approx 194.4$ THz. The incident drive field is polarized (s polarization) along the principal dipole axis of the rods, which themselves are oriented to match a high-Q TE-polarized mode of the microtoroid. The response measurements on the array involve a high-NA objective (NA ≈ 1.33, used with index-matching oil) operated in reflection. Focusing the incoming laser beam onto the back focal plane (BFP) of the objective gives precise control over the angle of incidence of the drive field. For scatterers arranged in a periodic array, scattering takes the form of diffraction into well-defined angles [wave vectors, Fig. 2(b)]. We discard the (-2) and (-1) diffraction orders propagating back into the substrate using Fourier filtering such that our detector is only sensitive to the specular reflection signal. In addition we employ a real-space filter, selecting a circular area of ~ 4.5 μm in diameter, to reduce background signals not originating from antennas coupled to the cavity. To illustrate this experimental arrangement, Fig. 2(c) displays an overlay of Fourier-space data obtained by BFP imaging (without Fourier filter). We identify (1) the radiation profile of the two propagating cavity modes, obtained by direct excitation of the cavity using an evanescently coupled tapered fiber (color scale), and (2) the position of the three diffraction orders of the array (indicated by arrows). The incoming wave vector ($k_{||}/k_0 = 0.84$) is chosen such that the (-2) diffraction order of the array (which is evanescent in air) overlaps with one of the propagating whispering gallery modes in the microtoroid, allowing the incoming field to efficiently scatter to the cavity mode via the antennas. Our system thus allows for a proper backaction measurement: the antennas can couple to the cavity, yet the detected signal is exclusively a probe of antenna polarizability. Any change in

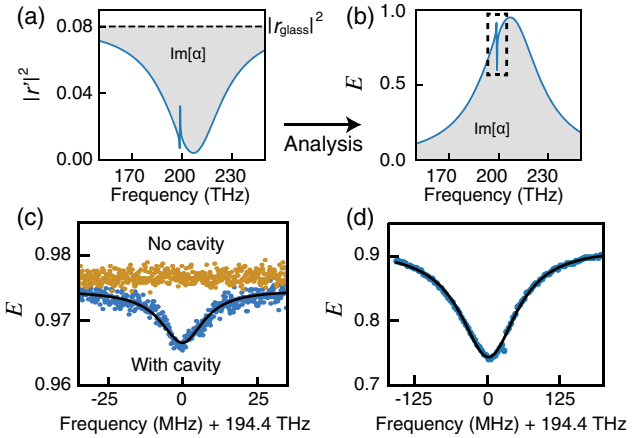

FIG. 3. (a) Sketch of a typical reflectance signal $|r'|^2$ as measured in the experiment. The plasmon feature introduces a broadband dip, with respect to the nonresonant $|r_{\mathrm{glass}}|^2$ value. (b) Sketch of the extinction E, obtained from (a). We expect the cavity mode to reduce the antenna extinction (and thus E) in a narrow frequency band. Dashed box: experimentally accessible frequency regime. (c),(d) Experiment. (c) With the cavity present (blue points), the extinction E decreases by 1% at the cavity frequency, a feature that is absent without cavity (orange points). (d) At smaller cavity-array distance the dip increases to 25%, indicating a strong suppression of antenna extinction. The cavity linewidth increases compared to (c) as a result of increased cavity losses.

detected signal upon approaching the cavity can thus be directly attributed to cavity-mediated backaction fields that renormalize the antennas' response.

In the experiment we probe the antennas through zero-order reflectance at a small (around 30 degree) incident angle, where zero-order reflectance is a direct measure of extinction, i.e., $\mathrm{Im}[\alpha]$ [32]. Since extinction is usually associated to zero-order transmittance and not reflectance, this claim requires substantiation. The antennas lie on a glass-air interface which in itself is reflective. To predict the line shape in reflectance, we quote an expression from de Abajo [23] for the near-normal incidence specular reflection r' of particle arrays

$$r' = r_{\mathrm{glass}} + \frac{2\pi i k \alpha}{A}, \tag{1}$$

where A is the unit-cell area of the array, k the wave number and α the antenna polarizability [33]. Importantly, one expects a reflection baseline given by the glass-air interface (nonresonant, real-valued r_{glass}) together with a broadband plasmon feature. One can show [24] that in our system the plasmon feature leads to a broadband reflectance *minimum* that primarily reports on $\mathrm{Im}[\alpha]$ [Fig. 3(a)]. In essence, destructive interference causes a reduction in reflectance, similar to the textbook scenario of extinction measurements that measure destructive interference between forward scattered light and the direct beam. In analogy to standard transmittance measurements probing extinction, we here identify the extinction E via $E \equiv 1 - |r|^2$, with the normalized reflectance $|r|^2$ given by $|r|^2 \equiv |r'|^2/|r_{\mathrm{glass}}|^2$. The use of $|r|^2$ has the advantage that results obtained at different excitation angles (leading to different values of r_{glass}) are more easily compared. Moreover, the introduction of the variable E simplifies the interpretation of our experiment: a decrease in antenna extinction (increasing $|r|^2$) is mapped to decreasing values for E. Our prediction is that the polarizability will show a reduction over a narrow spectral region [8,18], which will hence also appear as a minimum in E [Fig. 3(b)], once the antennas are subject to backaction through the cavity mode, i.e., once they are offered the additional possibility of radiation damping due to the Purcell factor associated with the cavity mode.

Figure 3(c) displays the response of the antenna array in absence (orange points) and presence (blue points) of the cavity for an incident beam with $k_{\parallel}/k_0 = 0.84$. The narrow frequency window displayed in Fig. 3(c) is close to the plasmon resonance. This is evident from the fact that E is close to unity, meaning that $|r|^2$ is close to zero. Comparing the trace without cavity and with the cavity approached to several microns distance away (antennas weakly couple to the cavity) shows a small backaction effect of the cavity on the array, visible as a $\sim$1% dip in E. This dip is tantamount to a *reduction* in the extinction that the antennas cause when they are offered the cavity as an additional channel to radiate into. Expressed in polarizability, our measurement implies a change in $\mathrm{Im}[\alpha]$ due to backaction, occurring over a narrow bandwidth that is commensurate with the linewidth of the high-Q cavity mode. In Fig. 3(c) the cavity-array distance was several microns, limiting the backaction experienced by the antennas. Moving the cavity closer to the array results in much larger effects. For instance, Fig. 3(d) shows a $> 25\%$ change in polarizability when approaching the cavity to within approximately 1 micron (about 4 times the evanescent decay length of the mode) from the antennas. This is direct evidence that the *magnitude* of polarizability can be substantially controlled by the photonic environment.

While our experiment probes several antennas, it was previously realized that for single antennas the polarizability modification must be directly linked to the cavity Purcell factor at the location of the antenna [8,18]. In other words, one viewpoint on our experiment is that it evidences that the polarizability of a nanoantenna is modified, which is mathematically expressed as $\alpha^{-1} = \alpha_0^{-1} - G$, with $\mathrm{Im}[G]$ the LDOS and $\mathrm{Re}[G]$ the Lamb shift [34] provided by the cavity mode. As such, an antenna is analogous to a quantum emitter in the sense that it probes the LDOS of the cavity. The effect of an LDOS peak, however, is distinctly different: the antenna emission is quenched on resonance rather than, as would be the case for an emitter, enhanced.

The fact that in our experiment the mode density provided by the cavity results from a single Lorentzian mode offers an alternative viewpoint. In essence, the reduction of polarizability over the cavity bandwidth can be viewed as a

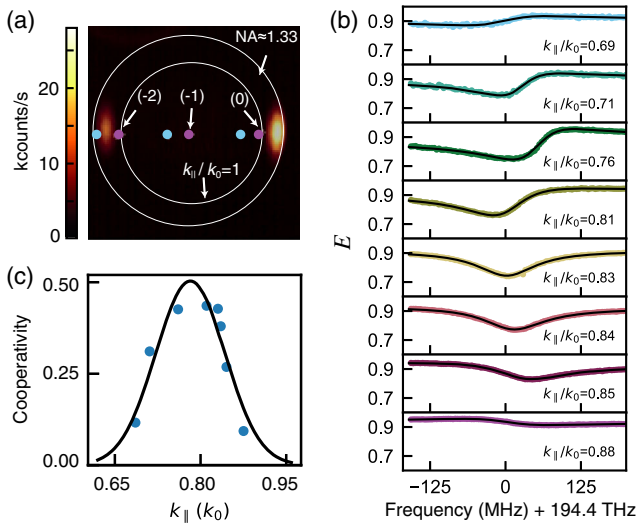

FIG. 4. (a) Fourier-image overlay that shows the position of the diffraction orders at the start (blue dot, $k_{||} = 0.69k_0$) and stop (pink dot, $k_{||} = 0.88k_0$) values of the $k_{||}$ sweep displayed in panel (b). (b) The strength and line shape of the backaction strongly depend on the incoming angle. The black lines are fits of our coupled-mode model. (c) Values for the cooperativity obtained from fitting our coupled-mode model to the spectra in panel (b). Black line: fit with a Gaussian line shape.

"transparency" feature in direct analogy to electromagnetically, plasmon, or optomechanically induced transparency [10,35–38]. In these systems, a broad resonator (here: plasmonic scatterer) is rendered "transparent" in its susceptibility to driving over a narrow frequency band due to coupling to a narrow resonator (here: WGM resonator), even though that narrow resonator is not directly driven. Beyond purely Lorentzian transparency dips, one can obtain Fano-type [39] line shapes depending on the phase of the coupling constants that connect the broad and narrow resonance. Inspired by this analogy we explore the shape of the backaction feature by varying the angle of incidence of the incoming drive field. As shown in Fig. 4(a), this effectively sweeps the (−2) diffraction order over the finite k-space width of the cavity mode, thus varying the degree to which the array and the cavity mode are coupled. From the resulting spectra [Fig. 4(b)] we qualitatively observe a dependence of the backaction strength and line shape on the incoming angle, which is expressed as a varying depth and asymmetry of the cavity-induced dip. In line with the phase-matching argument, visual inspection of Figs. 4(a) and 4(b) shows that cavity-mediated backaction is most prominent when the cavity mode profile and the (−2) diffraction order of the array experience better overlap. This behavior is verified using analytical coupled dipole calculations [24].

Full quantification of the backaction is not straightforward, as it requires analysis of the Fano line shapes. A detailed multiple scattering analysis particular for our system [24] shows that the plasmon antennas in our experiment are simultaneously subject to the resonant backaction of the cavity and a nonresonant backaction term from the interface on which the antennas are placed (glass-air) [3,40]. The nonresonant backaction is governed by the complex Fresnel coefficient associated with the interface, which exhibits a phase change for the (evanescent) (−2) diffraction order upon sweeping $k_{||}/k_0$. In our experiment we measure the scatterers' response in the presence of all backaction, which is a coherent sum of the broadband interface-induced backaction plus the resonant cavity-mediated backaction. Sweeping $k_{||}$ thus directly affects the Fano line shape that we observe. We develop a simple model based on coupled-mode theory [41] that can disentangle the resonant backaction from the nonresonant background. Treating the array and cavity as resonators, coupled at rate g, both described by a Lorentzian response with complex field amplitudes a and c, respectively, we solve the driven system

$$\begin{pmatrix} \Delta_a + i\gamma/2 & g \\ g & \Delta_c + \mathrm{i}\kappa/2 \end{pmatrix} \begin{pmatrix} a \\ c \end{pmatrix} = \begin{pmatrix} i\sqrt{\gamma_{\mathrm{ex}}} s_{\mathrm{in}} \\ 0 \end{pmatrix} \quad (2)$$

for a. Here we defined $\Delta_a \equiv \omega - \omega_a$ and $\Delta_c \equiv \omega - \omega_c$, where ω is the frequency of the incident field s_{in} driving the array and γ_{ex} the rate at which the array and input-output channel are coupled. Next, we use the input-output relation $s_{\mathrm{out}} = s_{\mathrm{in}} - \sqrt{\gamma_{\mathrm{ex}}} a$ [41] (such that $r = s_{\mathrm{out}}/s_{\mathrm{in}}$) and parameterize the coupling via the cooperativity $C = 4g^2/(\gamma\kappa)$, the determining quantity for the strength of the sharp spectral feature observed in electromagnetically or optomechanically induced transparency [42,43]. We obtain

$$|r|^2 = \left| \exp(i\phi) - \frac{2\eta}{1 + \frac{C}{\frac{2(\Delta_c - \Delta)}{i\kappa} + 1}} \right|^2, \quad (3)$$

where $\eta \equiv \gamma_{\mathrm{ex}}/\gamma$, Δ an additional small detuning that captures small fluctuations in ω_c due to e.g. thermal drift, ϕ an arbitrary phase pickup and we assumed $\omega \approx \omega_a$. We use Eq. (3) to fit [44] our experimental data in Fig. 4(b), yielding values for C as a function of $k_{||}$ [Fig. 4(c), blue points]. A Gaussian line shape (black line) is fit [center (width): $k_{||}/k_0 \approx 0.78$ (0.14)] to the blue data points, giving a maximum cooperativity of $C \approx 0.5$. Notably, the width and center of the Gaussian agree with expected values based on a crosscut of the cavity mode profile observed in Fig. 4(a). The cooperativity in the limit of a *single* scatterer and single cavity mode, is directly equivalent to the product of the scatterer albedo (A) and the cavity Purcell factor (F) at the location of the scatterer [24]. In our experiment the cooperativity cannot be directly cast into a Purcell factor, as we probe an array of antennas at specific wave vector, meaning that we probe a lattice-sum dressed polarizability (see de Abajo [23]) that experiences backaction from a wave vector resolved mode density. Using calculations on a lattice of scatterers [24], we estimate that the measured cooperativity of $C = 0.5$ actually corresponds to a value of $C = 1.7$ as it is felt by a single antenna, without a

lattice, located at the lattice origin. Considering that $A < 1$, the backaction feature in our experiment is tantamount to a modest Purcell factor of $F \geq 1.7$. Obviously this effect could be much stronger in experiments where the scatterers are placed right in the mode maximum, as opposed to the arrangement in our set up where scatterers are placed in the evanescent tail (estimated field decay length of 290 nm [24]) of the cavity mode at approximately 1 μm distance.

Concluding, we have shown that cavity backaction can alter the polarizability of an array of scatterers, and that the strength of the backaction can be controlled via the incoming drive field. Whereas in this work the Purcell enhancement provided by the cavity effectively depolarizes the nanorods, which is related to the fact that the cavity and array are nearly resonant, it has been predicted that both an increase and decrease in polarizability can be obtained by controlling the detuning between cavity and scatterers [18]. This type of control is instrumental for exploration of the field of hybrid cavity-antenna systems that promises to combine plasmonic field enhancements derived from scatterers with microcavity Qs with advantages for single-photon sources, strong coupling to single quantum emitters, as well as classical applications like single-molecule sensing [8,15,18,19,45]. Our results show the feasibility of such an approach.

We thank Martin Frimmer for stimulating discussions during the start of this project. This work is part of the research program of the Netherlands Organization for Scientific Research (NWO). A. F. K. acknowledges a NWO Vici grant.

F. R. and H. M. D. contributed equally to this work.

*f.koenderink@amolf.nl

[1] C. F. Bohren and D. R. Huffman, *Absorption and Scattering of Light by Small Particles* (John Wiley and Sons, New York, USA, 1983).
[2] P. de Vries, D. V. van Coevorden, and A. Lagendijk, Rev. Mod. Phys. **70**, 447 (1998).
[3] L. Novotny and B. Hecht, *Principles of Nano-Optics*, 2nd ed. (Cambridge University Press, Cambridge, UK, 2012).
[4] M. Agio and A. Alù, *Optical Antennas* (Cambridge University Press, Cambridge, UK, 2013).
[5] K. Drexhage, J. Lumin. **1–2**, 693 (1970).
[6] B. C. Buchler, T. Kalkbrenner, C. Hettich, and V. Sandoghdar, Phys. Rev. Lett. **95**, 063003 (2005).
[7] K. D. Heylman, N. Thakkar, E. H. Horak, S. C. Quillin, C. Cherqui, K. A. Knapper, D. J. Masiello, and R. H. Goldsmith, Nat. Photonics **10**, 788 (2016).
[8] M. Frimmer and A. F. Koenderink, Phys. Rev. B **86**, 235428 (2012).
[9] E. M. Purcell, Phys. Rev. **69**, 681 (1946).
[10] K. J. Boller, A. Imamoğlu, and S. E. Harris, Phys. Rev. Lett. **66**, 2593 (1991).
[11] R. Ameling and H. Giessen, Nano Lett. **10**, 4394 (2010).
[12] M. Barth, S. Schietinger, S. Fischer, J. Becker, N. Nüsse, T. Aichele, B. Löchel, C. Sönnichsen, and O. Benson, Nano Lett. **10**, 891 (2010).
[13] W. Ahn, S. V. Boriskina, Y. Hong, and B. M. Reinhard, ACS Nano **6**, 951 (2012).
[14] M. A. Schmidt, D. Y. Lei, L. Wondraczek, V. Nazabal, and S. A. Maier, Nat. Commun. **3**, 1108 (2012).
[15] Y.-F. Xiao, Y.-C. Liu, B.-B. Li, Y.-L. Chen, Y. Li, and Q. Gong, Phys. Rev. A **85**, 031805 (2012).
[16] R. Ameling and H. Giessen, Laser Photonics Rev. **7**, 141 (2013).
[17] M. R. Foreman and F. Vollmer, Phys. Rev. A **88**, 023831 (2013).
[18] H. M. Doeleman, E. Verhagen, and A. F. Koenderink, ACS Photonics **3**, 1943 (2016).
[19] B. Gurlek, V. Sandoghdar, and D. Martín-Cano, ACS Photonics **5**, 456 (2018).
[20] F. Ruesink, H. M. Doeleman, R. Hendrikx, A. F. Koenderink, and E. Verhagen, Phys. Rev. Lett. **115**, 203904 (2015).
[21] M. Husnik, S. Linden, R. Diehl, J. Niegemann, K. Busch, and M. Wegener, Phys. Rev. Lett. **109**, 233902 (2012).
[22] M. Husnik, J. Niegemann, K. Busch, and M. Wegener, Opt. Lett. **38**, 4597 (2013).
[23] F. J. García de Abajo, Rev. Mod. Phys. **79**, 1267 (2007).
[24] See Supplemental Material at http://link.aps.org/supplemental/10.1103/PhysRevLett.120.206101, which includes Refs. [25–30], for more information about our experiment and a discussion on Eq. (1). Moreover we present a multiple scattering analysis specific for our system and discuss the relation between albedo, Purcell factor and cooperativity.
[25] P. B. Johnson and R. W. Christy, Phys. Rev. B **6**, 4370 (1972).
[26] J. J. Penninkhof, L. A. Sweatlock, A. Moroz, H. A. Atwater, A. van Blaaderen, and A. Polman, J. Appl. Phys. **103**, 123105 (2008).
[27] C. M. Linton, SIAM Rev. **52**, 630 (2010).
[28] G. Anetsberger, Novel cavity optomechanical systems at the micro- and nanoscale and quantum measurements of nanomechanical oscillators, Ph.D. thesis, LMU München, 2010.
[29] K. M. McPeak, S. V. Jayanti, S. J. P. Kress, S. Meyer, S. Iotti, A. Rossinelli, and D. J. Norris, ACS Photonics **2**, 326 (2015).
[30] Y. Chen, Y. Zhang, and A. F. Koenderink, Opt. Express **25**, 21358 (2017).
[31] D. K. Armani, T. J. Kippenberg, S. M. Spillane, and K. J. Vahala, Nature (London) **421**, 925 (2003).
[32] H. C. van de Hulst, *Light Scattering by Small Particles* (John Wiley & Sons, New York, NY, 1957).
[33] Note that Eq. (8) in [23] uses a lattice-normalized polarizability.
[34] W. E. Lamb, Jr. and R. C. Retherford, Phys. Rev. **72**, 241 (1947).
[35] S. Zhang, D. A. Genov, Y. Wang, M. Liu, and X. Zhang, Phys. Rev. Lett. **101**, 047401 (2008).
[36] N. Liu, L. Langguth, T. Weiss, J. Kästel, M. Fleischhauer, T. Pfau, and H. Giessen, Nat. Mater. **8**, 758 (2009).
[37] S. Weis, R. Rivière, S. Deléglise, E. Gavartin, O. Arcizet, A. Schliesser, and T. J. Kippenberg, Science **330**, 1520 (2010).

[38] A. H. Safavi-Naeini, T. P. M. Alegre, J. Chan, M. Eichenfield, M. Winger, Q. Lin, J. T. Hill, D. E. Chang, and O. Painter, Nature (London) **472**, 69 (2011).
[39] U. Fano, Phys. Rev. **124**, 1866 (1961).
[40] A. Kwadrin, C. I. Osorio, and A. F. Koenderink, Phys. Rev. B **93**, 104301 (2016).
[41] H. A. Haus, *Waves and Fields in Optoelectronics* (Prentice Hall, Englewood Cliffs, NJ US, 1984).
[42] M. Aspelmeyer, T. J. Kippenberg, and F. Marquardt, Rev. Mod. Phys. **86**, 1391 (2014).
[43] P. Lodahl, S. Mahmoodian, and S. Stobbe, Rev. Mod. Phys. **87**, 347 (2015).
[44] See the Supplemental Material (Sec. IV) at http://link.aps.org/supplemental/10.1103/PhysRevLett.120.206101 for more fit results.
[45] F. Vollmer and L. Yang, Nanophotonics **1**, 267 (2012).